CHEMMEDCHEM

CHEMISTRY ENABLING DRUG DISCOVERY

Accepted Article

Title: Solid Phase Synthesis and Evaluation of Substrate-based Dipeptides and Heterocyclic Pseudo-dipeptides as Potential NO Synthases Inhibitors

Authors: Youness Touati-Jallabe, Thibault Tintillier, Elodie Mauchauffée, Jean-Luc Boucher, Jérémy Leroy, Booma Ramassamy, Abdallah Hamzé, Karima Mezghenna, Amine Bouzekrini, Claudia Verna, Jean Martinez, Anne-Dominique Lajoix, and Jean-François Hernandez

To be cited as: *ChemMedChem* 10.1002/cmdc.201900659

Link to VoR: http://dx.doi.org/10.1002/cmdc.201900659

A Journal of

ChemPubSoc Europe

WILEY-VCH

www.chemmedchem.org

FULL PAPER WILEY-VCH

Solid Phase Synthesis of Substrate-based Dipeptides and Heterocyclic Pseudo-dipeptides as Potential NO Synthase Inhibitors

Youness Touati-Jallabe,[a,b] Thibault Tintillier,[a,c] Elodie Mauchauffée,[a] Jean-Luc Boucher,[d] Jérémy Leroy,[e] Booma Ramassamy,[d] Abdallah Hamzé,[a,f] Karima Mezghenna,[e] Amine Bouzekrini,[e] Claudia Verna,[a] Jean Martinez,[a] Anne-Dominique Lajoix,*[e] and Jean-François Hernandez*[a]

[a] Dr. Y. Touati-Jallabe, Dr. T. Tintillier, Dr. E. Mauchauffée, Dr. A. Hamzé, C. Verna, Pr. J. Martinez, Dr. J.-F. Hernandez
Institut des Biomolécules Max Mousseron
CNRS, Université Montpellier, ENSCM
Faculté de Pharmacie, 34000 Montpellier, France
E-mail: jean-francois.hernandez@umontpellier.fr

[b] Dr. Y. Touati-Jallabe
Current address: Avara Pharmaceutical Services, Boucherville, QC J4B 7K8, Canada

[c] Dr. T. Tintillier
Current address: Asymptote Project Management, 1 rue Edisson, 69500 Bron, France

[d] Dr. J.-L. Boucher, B. Ramassamy
Laboratoire de Chimie et Biochimie Pharmacologiques et Toxicologiques
UMR8601, CNRS, Université Paris-Descartes
45 rue des Saints Pères, 75270 Paris Cedex 06, France

[e] J. Leroy, Dr. K. Mezghenna, A. Bouzekrini, Dr. A.-D. Lajoix
Centre Biocommunication en Cardio-métabolique
Université Montpellier
Faculté de Pharmacie, 34000 Montpellier, France
E-mail: anne-dominique.lajoix@umontpellier.fr

[f] A. Hamzé
Current address: BioCIS, UMR 8076, CNRS, Université Paris Sud, Université Paris-Saclay, Faculté de Pharmacie, 92296 Châtenay-Malabry, France

Supporting information for this article is given via a link at the end of the document.

Abstract: More than 160 arginine analogues modified on the C-terminus via either an amide bond or a heterocyclic moiety (1,2,4-oxadiazole, 1,3,4-oxadiazole and 1,2,4-triazole) were prepared as potential inhibitors of NO synthases (NOS). A methodology involving formation of a thiocitrulline intermediate linked through its side-chain on a solid support followed by modification of its carboxylate group was developed. Finally, the side-chain thiourea group was either let unchanged, *S*-alkylated (Me, Et) or guanidinylated (Me, Et) to yield respectively after TFA treatment the corresponding thiocitrulline, *S*-Me/Et-isothiocitrulline and *N*-Me/Et-arginine substrate analogues. They all were tested against three recombinant NOS isoforms. Several compounds containing a *S*-Et- or a *S*-Me-Itc moiety and mainly belonging to both the dipeptide-like and 1,2,4-oxadiazole series were shown to inhibit nNOS and iNOS with IC_{50} in the 1-50 μM range. Spectral studies confirmed that these new compounds interacted at the heme active site. The more active compounds were found to inhibit intra-cellular iNOS expressed in RAW264.7 and INS-1 cells with similar efficiency than the reference compounds L-NIL and SEIT.

Introduction

Nitric oxide (NO) is an important signaling molecule in the living kingdom.[1] In mammals, it is synthesized from L-Arginine (L-Arg) by nitric oxide synthases (NOS) comprising the neuronal, inducible and endothelial NOS distinct isoforms.[2] Neuronal NOS (nNOS) and endothelial NOS (eNOS) are constitutively expressed and mainly involved respectively in neurotransmission, and in smooth muscle relaxation, maintenance of blood pressure, platelet aggregation. nNOS is also expressed in pancreatic β-cells where it controls insulin secretion.[3] By contrast, inducible NOS (iNOS) is expressed by macrophages in response to pro-inflammatory cytokines, and contributes to the innate immune response.[4] The three NOS isoforms are composed of two domains: the *N*-terminal oxygenase domain containing the heme prosthetic group and the binding site for the substrate L-Arg, and the C-terminal reductase domain. The two domains are connected by a calmodulin binding sequence.[2,5-7]

Overproduction of NO is observed in several pathophysiological states and mainly concerns nNOS and iNOS.[8-12] Neuronal NOS is involved in stroke and neurodegenerative diseases,[13,14] while iNOS has been identified as the cause of or an aggravating factor in several human diseases involving an inflammatory state, including septic shock, chronic inflammatory diseases, insulin resistance, cancers, migraine.[15-20] Thus, nNOS and iNOS are potential therapeutical targets, but the multiple roles of NO complicate the discovery of inhibitors of pharmaceutical interest.[21] In particular, such inhibitors must be highly selective to preserve the essential eNOS functions. The crystal structure of the three NOS oxygenase domains (NOSoxy) has shown a very strong conservation of the heme active site and substrate binding site residues.[22-25] Because of this striking similarity, selective inhibition of a NOS isoform is highly challenging. Several successes have been reached in the case of nNOS.[26,27] In particular, the original strategy proposed by R. B. Silverman was to attach, via an amide bond, an extension to the C-terminus of a substrate-based and poorly selective inhibitor (i.e. L-N^{ω}-nitro-Arginine).[28] The extension can establish selective

interactions with residues of the less conserved substrate-access channel. This strategy led to compounds exhibiting >1000-fold selectivity toward nNOS over eNOS). X-Ray analysis of co-crystal complexes of these inhibitors with nNOS and eNOS allowed identification of the main sites inducing selectivity.[29] Based on these results, a computer modelling approach led to the design of new promising compounds.[30] In the case of iNOS, a few highly selective inhibitors have been reported. Amidine-type substrate analogues were shown to irreversibly inactivate iNOS in a time-dependent manner, whereas they behave as fast reversible inhibitors of the two other isoforms.[31-35] Combinatorial approaches identified pyrimidine-imidazole-based inhibitors of iNOS dimerization[36-37] and the spirocyclic quinazoline AR-C102222. The causes of selectivity were also established by X-ray crystallography.[38] To date, despite a huge amount of studies, no NOS inhibitor was shown to be clinically useful because some parameters (toxicity, bioavailability, etc…) have prevented their therapeutic use.[39-41] For instance, efforts are still in progress to improve the permeability of nNOS inhibitors.[42-44] Therefore, developing a clinically useful NOS inhibitor remains a strong challenge.

In this context, we have developed dipeptide mimetic compounds following Silverman's strategy from different substrate-based inhibitors, i.e. thiocitrulline (Tci), *S*-alkyl-isothiocitrullines (Itc) and *N*-alkyl-arginines (Figure 1).[45-48] Whereas few *S*-alkyl-L-isothiocitrulline-containing dipeptides were previously reported as human iNOS moderate selective inhibitors,[49-50] no extensive development of these series was undertaken yet. We first synthesized a library of thiocitrullines, *S*-alkyl-L-isothiocitrullines and *N*-alkyl-arginines modified on their C-terminus via an amide bond (dipeptide-like). We also replaced the amide bond by 1,2,4- and 1,3,4-oxadiazoles and 1,2,4-triazoles heterocyclic structures considered as amide bond isosteric moieties. For their synthesis, we exploited a solid phase synthetic strategy following a side-chain anchoring approach.[51] This method allowed the easy and rapid synthesis of numerous compounds containing both substrate analogues from a single supported thiocitrulline intermediate, and possessed a high combinatorial approach potential.

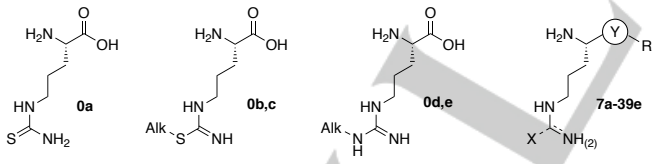

Figure 1. Structure of thiocitrulline (**0a**), *S*-alkyl-isothiocitrullines (**0b**, Alk = Me; **0c**, Alk = Et), *N*-alkyl arginines (**0d**, Alk = Me; **0e**, Alk = Et), and general structure of the target molecules (**7a-39e**; X = S=, Alk-S-, or Alk-NH-; Y = CO-NH, or heterocycle).

Results and Discussion

Chemistry.

- *Synthesis of the supported precursors.* All compounds were prepared from a single intermediate, a *N*α-Boc-protected thiocitrulline methyl ester linked to the solid support (a standard cross-linked polystyrene (PS) resin or a PS-loaded Synphase lantern from Mimotopes) through its thiourea group (compound **4**). The solid-supported intermediate **4** was synthesized in four steps from the ornithine derivative Boc-L-Orn(*N*$^{\delta}$-Z)-OH according to our previously described strategy (Scheme 1).[51] After formation of the methyl ester **1** using MeI, the Z protecting group was removed by catalytic hydrogenolysis in the presence of 1.5 equiv. TFA to trap the free δ-amino group and prevent its intramolecular reaction with the methyl ester. The resulting TFA salt **2** was converted into isothiocyanate **3** using CS_2 followed by desulfurization with H_2O_2.[52] Compound **3** was then loaded onto a Rink amide solid support to yield the protected thiocitrulline derivative **4** attached via its side-chain. The loading completion was assessed using the TNBS (trinitrobenzenesulfonyl) test. Finally, the methyl ester **4** was either hydrolysed with LiOH in a mixture of THF/H_2O (7/3)[53] yielding the intermediate **5** (precursor for dipeptide-like and 1,2,4-oxadiazole compounds), or treated with hydrazine hydrate in THF leading to hydrazide **6** (precursor for 1,3,4-oxadiazole and 1,2,4-triazole compounds).

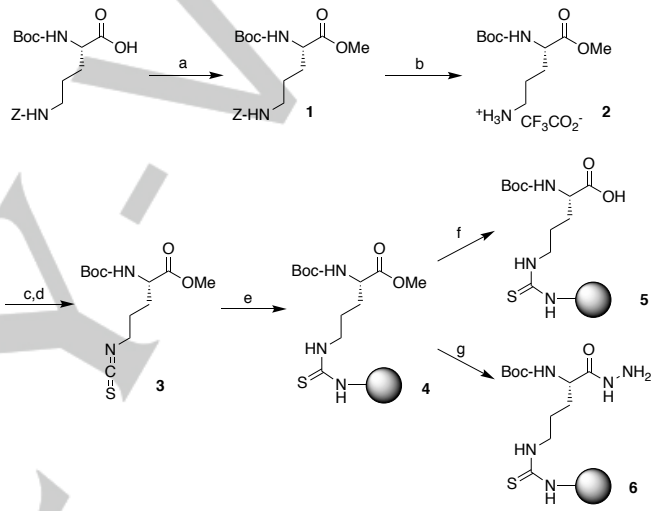

Scheme 1. Synthesis of the supported thiocitrulline intermediates **5** and **6**: (a) MeI, Na_2CO_3, DMF, rt, 5h; (b) H_2, 10% Pd/C, EtOH, 1.5 equiv. TFA, 4h; (c) CS_2, TEA, THF, 0 °C, 45 min; (d) H_2O_2, 30 min addition, then 5 min, 0 °C; (e) 3 equiv. **3**, Rink amide solid support, TEA, THF, 60 °C, 3h; (f) 5 equiv. LiOH, THF/water (7/3), rt, overnight; (g) 5 equiv. hydrazine hydrate, THF, rt, 24 h..

- *Solid phase synthesis of the inhibitors.* The efficiency of all synthetic strategies was checked on standard PS resin and allowed the fast synthesis of several series of compounds possessing a variable linker. In addition, in the case of dipeptide-like and 1,2,4-oxadiazole-containing analogues, two libraries were prepared on Synphase lanterns (Mimotopes, Australia). Thanks to color tagging, the advantage of these solid support units was to perform common steps (i.e. *S*-alkylation, guanidinylation, see below) in only one batch for all compounds. Two 35 μmol-loaded PS lanterns possessing a Rink amide spacer were used for the synthesis of each compound.

- *Dipeptide-like inhibitors.* The preparation of the dipeptide-like compounds on either PS resin or lanterns is presented in Scheme 2. The thiocitrulline intermediate **5** was coupled to various amines using BOP and HOAt in the presence of DIEA to yield the corresponding supported dipeptide-like intermediates. Each intermediate was divided into five samples. One sample was cleaved with TFA to give Tci-containing analogues **7a-22a**. Another sample was reacted with MeI leading to *S*-Me-Itc-containing analogues **7b-21b** after cleavage from the solid

support. A similar treatment was performed on another sample with EtI yielding *S*-Et-Itc-containing analogues **7c-22c** after cleavage. Finally, the last two samples were first *S*-methylated and then guanidinylated using either methylamine or ethylamine, respectively giving the series of *N*-Me-Arg- and *N*-Et-Arg-containing analogues **7d-21d** and **7e-21e** after cleavage. Seventy-six compounds (16 different extensions x 5 substrate analogues with the exception of **12e**, **22b**, **22d** and **22e**, which could not be obtained in sufficient amounts) have been prepared (see Table 1). In addition, the five substrate-based amino acids (**0a-e**) were similarly prepared from **4**, the methyl ester being removed just before acidic cleavage (not shown).

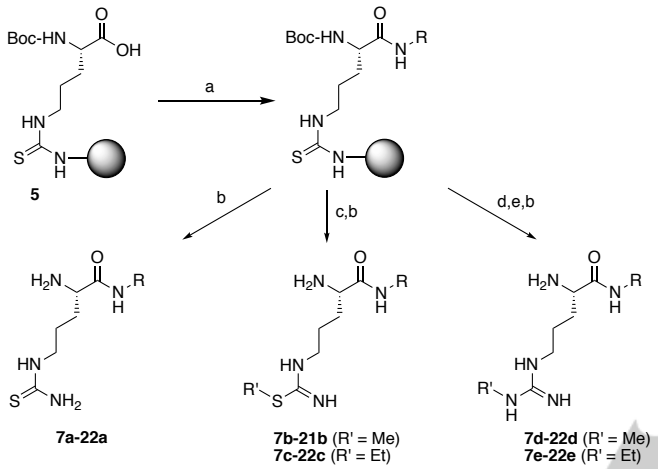

Scheme 2. Synthesis of the Tci- (**7a-22a**), *S*-alkyl-Itc- (**7b-21b**, **7c-22c**) and *N*-alkyl-Arg- (**7d-21d**, **7e-22e**) containing dipeptide-like inhibitors: (a) 1.3 equiv. H_2N-R, BOP, HOAt, 1.5 equiv. DIEA, DMF, rt, 5h, repeated twice; (b) TFA/TIS/$H_2$0 (95:2.5:2.5), rt, 1.5 h, excepted *S*-alkyl-Itc analogues: 40 °C, 2h; (c) **7b-21b**: 0.2 M MeI in DMF, rt, 3x1h; **7c-22c**: 0.2 M EtI in DMF, 50 °C, 3x1h (d) 0.2 M MeI in DMF, rt, 3x1h; (e**) 7d-21d**: 2 M $MeNH_2$,HCl and 2 M NMM in anhydrous DMSO, 80 °C, 15h; **7e-21e**: 2.5 M $EtNH_2$,HCl and 2.5 M NMM in anhydrous DMSO, 80 °C, 15h.

- *Dipeptide mimetics with a heterocyclic link.* Several series of compounds containing a 5-atoms heterocyclic link (i.e. 1,2,4- and 1,3,4-oxadiazoles, 1,2,4-triazole) were considered. The presence of such heterocyclic structure could increase the metabolic stability as well as the bioavailability, compared to the amide-containing analogues. In addition, their higher rigidity might help to obtain NOS isoform selective inhibitors. These heterocycles contain an extra heteroatom compared to the amide bond, which could establish an additional hydrogen bond in the enzyme binding site. Although the three heterocyclic moieties are similar in size and shape and present the two substituents in very similar positions, they show variations in aromatic, electrostatic, and hydrogen bonding properties. This could lead to different binding modes with the target, and therefore to variation in inhibitory potencies between compounds only differing by the heterocyclic moiety.[54,55]

Fourty-four 1,2,4-oxadiazole derivatives were synthesized and the specific synthetic steps of their preparation on standard resin and Synphase lanterns are shown in Scheme 3.

Intermediate **5** was coupled to various amidoximes using DIC/HOBt. The intermediates were then cyclo dehydrated by adapting mild conditions (80 °C and no strong base) that we previously described for the solution synthesis of 1,2,4-oxadiazole compounds from Fmoc-protected aspartyl derivatives.[56] Indeed, we found that sodium acetate strongly accelerated the cyclo dehydration step. The same was true on the solid phase and a THF/water mixture was used to keep a good resin swelling. Two cycles of coupling/cyclo dehydration were generally sufficient for complete conversion. Finally, the supported thiocitrulline intermediates were treated as described above to yield the five substrate analogues. HPLC analyses of the crude products obtained after cleavage generally showed a major peak with at least 80% purity (Figures S1 and S2).

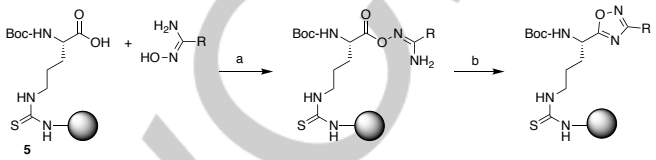

Scheme 3. Key steps in the synthesis of the Tci- (**23a-31a**), *S*-alkyl-Itc- (**23b-31b**, **23c-31c**) and *N*-alkyl-Arg- (**23d-31d**, **23e-31e**) based 1,2,4-oxadiazole-containing inhibitors: (a) 1.3 equiv. amidoxime, HOBt, DIC, NMP, rt, 4h; (b) 1.2 equiv. AcONa, THF/water (7/3), reflux, overnight. Steps a and b were repeated one more time.

We also synthesized a few examples of 1,3,4-oxadiazole (13 compounds) and di-substituted 1,2,4-triazole (25 compounds) derivatives. They were prepared on a standard cross-linked PS resin from the hydrazide precursor **6** (Scheme 4).

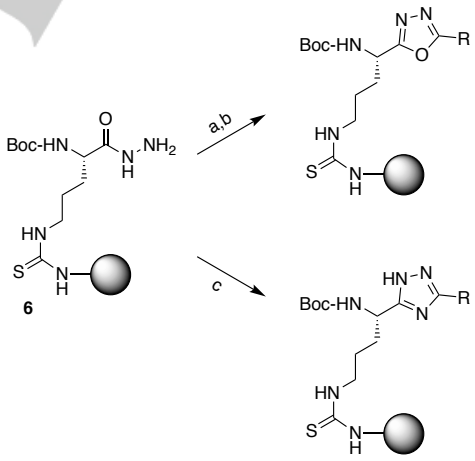

Scheme 4. Key steps in the synthesis of the Tci- (**32a-34a** and **35a-39a**), *S*-alkyl-Itc- (**32b-34b** and **35b-39b**, **32c-34c** and **35c-39c**) and *N*-alkyl-Arg- (**32d-34d** and **35d-39d**, **32e-34e** and **35e-39e**) containing 1,3,4-oxadiazole- and 1,2,4-triazole-based inhibitors. [a]Reagents and conditions: (a) 3 equiv. R-CO_2H, 3 equiv. HBTU, 4 equiv. DIEA, DMF, 4 h; (b) 2.6 equiv. C_2Cl_6, 10 equiv. DIEA, anhydrous MeCN, 5 min then 4 equiv. PPh_3, rt, 30 min. Steps i and ii were repeated once more. (c) 5 equiv. R-C(=NH)NH_2 or R-C(=NOH)NH_2, reflux 24 h.

For the 1,3,4-oxadiazole compounds, the hydrazide was coupled to three different carboxylic acids, followed by cyclo dehydration in the presence of C_2Cl_6 and PPh_3.[57] The five substrate analogues were then prepared as described above. These compounds were obtained in moderate yields after purification. The cyclisation was not complete and we observed formation of a side product probably resulting from the conversion of the thiourea group to urea as suggested by LC-MS analysis. This

compound remained unchanged through the following steps (*S*-alkylation and guanidinylation). However, about 70% of the expected derivative was present in the crude after cyclisation (Figure S3).

For the synthesis of 1,2,4-triazole compounds substituted at positions 3 and 5, we first reacted hydrazide **6** with benzamidine.[58] After 24h reflux in 2-methoxyethanol, the condensation to the acylamidrazone intermediate followed by cyclo dehydration proceeded cleanly and totally (Figure S4A). However, this approach was limited by the access to various amidines. So, we checked if the close and more easily accessible amidoxime derivatives, which were used in the synthesis of 1,2,4-oxadiazole analogues could replace amidines. Indeed, the reaction of resin **6** with the corresponding benzamidoxime in the same experimental conditions led to similar results (Figure S4B). To our knowledge, the use of amidoximes for the synthesis of di-substituted 1,2,4-triazoles has never been described. Therefore, we followed this synthetic pathway using four more amidoximes and 25 compounds were obtained.

The completion of each reaction was checked by LC-MS analysis after cleavage of a small portion of the solid support (resin or lantern). Whereas the linkage between the thiourea group of Tci and the Rink amide support was found to be TFA labile, the one involving the *S*-alk-Itc residues was much more resistant. A prolonged TFA treatment and light warming were necessary to cleave *S*-alk-Itc from the solid support. All compounds were obtained in low to moderate yields (5-50%) after purification (reverse-phase HPLC).

Biological evaluation.

- *Inhibition of NO Synthases.* The inhibitory effects of all compounds were evaluated against the formation of NO by three recombinant NOSs (mouse iNOS, rat nNOS, and bovine eNOS) on 96-wells plates using the oxyhemoglobin test.[59] A first screening at 100 and 10 μM was performed and the IC_{50} were measured for compounds showing more than 50% inhibition at 100 μM (Tables 1 to 4).

The five α-amino acids **0a-e** are all potent inhibitors of the three NOSs, with IC_{50} values in the low micromolar range (Table 1), close to those reported in the literature.[48,60,61]

In the dipeptide-like series (Table 1), compounds possessing two main types of extension displayed significant activities against at least one NOS (IC_{50} in the 2-50 μM range). The first one contained an alkylamine moiety preferentially with a propyl (**7a-c**) but also a butyl (**8c**) chain. Increasing the chain length by one more CH_2 (pentyl) led to inactive compounds (**9** series) indicating that the propyl chain was optimal. This result was expected as Huang et al.[62] reported that the corresponding analogue Arg($N^{\omega}NO_2$)-NH-$(CH_2)_3$-NH_2 inhibited nNOS with a K_i of 0.46 μM. These authors proposed that the amine group establishes a significant ionic interaction within the substrate access channel. However, this compound was much more selective toward iNOS and eNOS (> 200-fold selectivity) than **7c** that was only 10- and 18-fold more selective against iNOS and eNOS respectively. The second most favorable extension was the furfuryl group with **21c** being moderately active on both NOSs. Apart some exceptions for nNOS (**11c**, **12b/c**, **14b**, and **22c**), all other more or less bulky aromatic substituents did not lead to any significant inhibitor. In the dipeptide-like series, small substituents on the amide bond and an *S*-Et-Itc moiety were preferred.

In the 1,2,4-oxadiazole series (Table 2), a small substituent was also favorable to the inhibition of the three NOS (**23b** and **23c**). The methyl group was probably too small to establish any significant interaction with the enzymes, suggesting that the 1,2,4-oxadiazole heterocycle could indeed interact favorably. The micromolar activity of other compounds (**25c**, **26c**, **27c**, **29b**, **29c**, **31c**) indicates that in this series, the enzymes could accommodate bulky aromatic substituents.

The 1,3,4-oxadiazole series (Table 3) contains only three different substituents. As in the 1,2,4-oxadiazole series, a methyl substituent led to significant inhibition but surprisingly with a *N*-Et-Arg (**32e**). All other compounds were found inactive with the exception of the *S*-Et-Itc analogue **34c**.

Finally, **in the 1,2,4-triazole series** (Table 4), the methyl group was moderately favorable for iNOS and nNOS inhibition (**35c**). Among other analogues, only **37b**, **37c** and **38c** showed moderate inhibition of nNOS and/or iNOS.

As a general observation, modification of the α-carboxylic group of the substrate analogues resulted in the loss of important stabilizing interactions and most of the compounds showed no significant (< 50% inhibition at 100 μM) or modest inhibitory activity in the 10-50 μM range, except for compounds **7b** and **7c** that bore a NH_2-group at the end of a short flexible chain, and for the 1,2,4-oxadiazole derivatives **23b** and **23c** having a short extension. This low activity could be explained by poor interaction(s) of the moiety replacing the α-COOH group in the substrate access channel. The steric hindrance was also clearly an unfavorable factor for binding to the NOSs, but the introduction of polar substituents (e.g. OH, COOH in **12b**, **29b**) on the extension could restore some interaction(s), probably with residues in the substrate access channel. Although the five α-amino acids **0a-e** were all potent inhibitors of the three enzymes, the most active compounds belonged to the *S*-Et-Itc series, indicating that this substrate analogue made sufficient stabilizing interactions at the active site to compensate the loss of the carboxylic function, and/or favors the extension interactions within the substrate access channel. The X-ray structure of the complex of human iNOS and *S*-ethylisothiourea (SEIT) has shown that the ethyl group packed near the heme and Phe^{369} side-chain and appeared optimal for interacting with the NOS distal cavity.[23] iNOS almost exclusively preferred *S*-Et-Itc (for instance, **7c**, **8c**, **21c**, **23c**, **25c**, **26c**, **27c**, **34c**, **35c**, **38c**, with IC_{50} from 7.2 to 45 μM) with very few exceptions in the *S*-Me-Itc series (**7b** and **23b**, with IC_{50} of 7.0 and 23.9 μM, respectively) and only one example in the Tci and *N*-Et-Arg series (**7a** and **32e**, respectively).

In the case of nNOS, *S*-Et-Itc and *S*-Me-Itc were also the most favorable substrate analogues (for instance, **7b**, **7c**, **8c**, **11c**, **12b**, **12c**, **14b**, **21c**, **22c**, **23b**, **23c**, **27c**, **29b**, **29c**, **31c**, **34c**, **35c**, **37c**, **38c**, with IC_{50} from 0.4 to 42.0 μM) with the exception of the Tci analogue **7a** and the *N*Et-Arg analogue **32e**. Finally, only a few compounds significantly inhibited eNOS (**7a**, **7b**, **21c**, **23b**, **23c**, **32e**, **35c**, **37c**, with IC_{50} from 1.4 to 44.9 μM), but also inhibited nNOS and iNOS, indicating that eNOS was less easily inhibited by this type of compounds. This result is in agreement with the studies published by Park et al.[50] and Huang et al.[28] about few *S*-Me-Itc- and *S*-Et-Itc-containing dipeptides, and Arg(N^{ω}Nitro)-containing dipeptides, respectively.

Table 1. Structures of amino acids **0a-e** and dipeptide-like compounds **7**-**22** and *in vitro* NOS inhibition (IC_{50} in μM)[a]

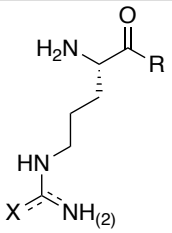

Cpds	R	Series	X	IC_{50} (μM) (or % inhibition at 100 μM)		
				iNOS (Mouse)	nNOS (Rat)	eNOS (Bovine)
0	-OH	a	S=	5.1	1.45	5.0
		b	Me-S-	2.2	0.23	0.8
		c	Et-S-	2.9	0.64	3.1
		d	Me-NH-	21.9	2.9	3.5
		e	Et-NH-	4.1	4.5	4.5
7	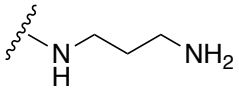	a	S=	41.8	10.0	12.5
		b	Me-S-	7.0	0.4	1.4
		c	Et-S-	47.9	6.6	52.4
		d	Me-NH-	NI	NI	NI
		e	Et-NH-	61.6	33.3	19.8
8	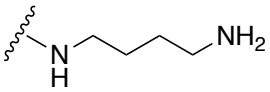	a	S=	NI	NI	NI
		b	Me-S-	NI	NI	NI
		c	Et-S-	17.0	21.7	56.6
		d	Me-NH-	NI	NI	NI
		e	Et-NH-	NI	NI	NI
9	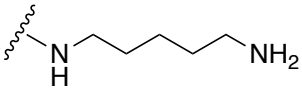	a	S=		NI	
		b	Me-S-		53% at 100 μM	
		c	Et-S-	All NI	NI	All NI
		d	Me-NH-		NI	
		e	Et-NH-		NI	
10	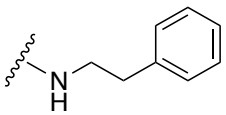	a	S=	NI		
		b	Me-S-	NI		
		c	Et-S-	90.0	All NI	All NI
		d	Me-NH-	NI		
		e	Et-NH-	NI		
11	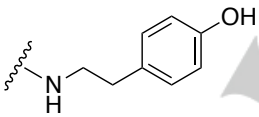	a	S=	NI	NI	
		b	Me-S-	NI	45% at 100 μM	
		c	Et-S-	75.3	32.5	All NI
		d	Me-NH-	NI	NI	
		e	Et-NH-	NI	NI	
12	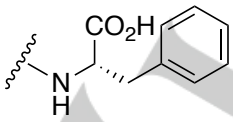	a	S=	ND[b]	NI	NI
		b	Me-S-	45% at 100 μM	9.6	45.2
		c	Et-S-	70% at 100 μM	23.0	NI
		d	Me-NH-	NI	NI	NI
13	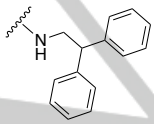	a	S=			
		b	Me-S-			
		c	Et-S-	All NI	All NI	All NI
		d	Me-NH-			
		e	Et-NH-			
14	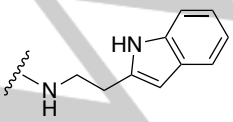	a	S=		NI	
		b	Me-S-		18.6	
		c	Et-S-	All NI	45% at 100 μM	All NI
		d	Me-NH-		NI	
		e	Et-NH-		NI	

15	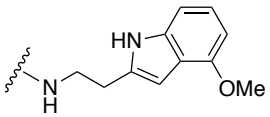	a	S=		NI	
		b	Me-S-		26.6	
		c	Et-S-	All NI	45% at 100 μM	All NI
		d	Me-NH-		NI	
		e	Et-NH-		NI	
16	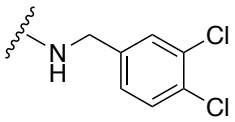	a	S=			
		b	Me-S-			
		c	Et-S-	All NI	All NI	All NI
		d	Me-NH-			
		e	Et-NH-			
17	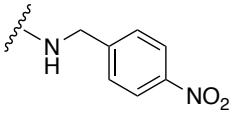	a	S=			
		b	Me-S-			
		c	Et-S-	All NI	All NI	All NI
		d	Me-NH-			
		e	Et-NH-			
18	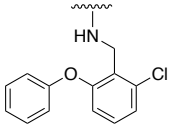	a	S=			
		b	Me-S-			
		c	Et-S-	All NI	All NI	All NI
		d	Me-NH-			
		e	Et-NH-			
19	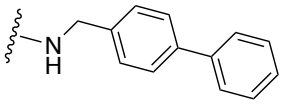	a	S=		NI	
		b	Me-S-		45% at 100 μM	
		c	Et-S-	All NI	55% at 100 μM	All NI
		d	Me-NH-		NI	
		e	Et-NH-		NI	
20	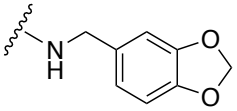	a	S=			
		b	Me-S-			
		c	Et-S-	All NI	All NI	All NI
		d	Me-NH-			
		e	Et-NH-			
21	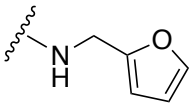	a	S=	NI	NI	NI
		b	Me-S-	NI	NI	NI
		c	Et-S-	19.1	16.9	27.6
		d	Me-NH-	NI	NI	ND
		e	Et-NH-	NI	NI	ND
22	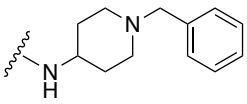	a	S=		NI	
				All NI		All NI
		c	Et-S-		40.0	

[a]NI = no significant inhibition (<50% at 100 μM). [b]ND = not determined.

Some inhibitors showed moderate (10-20-fold) selectivity for nNOS against iNOS. This was the case for **7b** (IC_{50} of 0.4 and 7.0 μM, respectively), **7c** (IC_{50} of 6.6 and 47.9 μM, respectively), **23b** (IC_{50} of 2.0 and 23.9 μM, respectively), and **29b** (IC_{50} of 3.2 μM and NI, respectively). Compound **7c** was also 8-fold selective against eNOS. The 1,2,4-oxadiazoles **25c**, **26c** and **31c**, and the 1,3,4-oxadiazole **34c** showed moderate selectivity (≥ 3-fold) in favor of iNOS vs nNOS and eNOS. In particular, **25c**, which contains a branched extension, did not inhibit nNOS at 100 μM, indicating that this bulky substituent was not favorable for nNOS inhibition.

One interesting point was to assess the importance of the link between the substrate analogue and the extension. For instance, it was possible to compare **23b** and **23c** (1,2,4-oxadiazoles) with, respectively, **32b** and **32c** (1,3,4-oxadiazoles), and **35b** and **35c** (1,2,4-triazoles), all bearing a methyl substituent on the heterocycle. We observed that the 1,2,4-oxadiazole ring (compounds **23b** and **23c)** was the most favorable for NOS inhibition with the 1,3,4-oxadiazole ring being the less efficient. In contrast, when comparing the 1,2,4-oxadiazole **30c** and the 1,2,4-triazole **38c** (*p*-nitrobenzyl), only **38c** showed inhibitory activity, the corresponding dipeptide-like analogue **17c** being also inactive. The dipeptide-like **11c**, the 1,2,4-oxadiazole **29c** and the 1,2,4-triazole **37c** (*p*-hydroxybenzyl) exhibited similar inhibitory potencies toward nNOS. Finally, 1,2,4-oxadiazoles **28a-e** and 1,2,4-triazoles **39a-e** (benzodioxol extension) exhibited either low or no activity, respectively. Although the number of examples was too low to establish a reliable ranking between the various links, the present results suggested that 1,2,4-oxadiazole and 1,2,4-triazole rings could be as favorable as the peptide bond. As stated above, the observed variation in inhibitory potencies between compounds only differing by the heterocyclic link probably originated from the different aromatic, electrostatic, and hydrogen bonding properties of the three heterocycles.[54,55]

Table 2. Structures of 1,2,4-oxadiazoles **23**-**31** and *in vitro* NOS inhibition (IC_{50} in μM)[a]

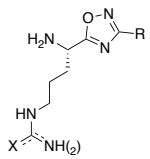

Cpds	R	Series	X	IC_{50} (μM) (or % inhibition at 100 μM)		
				iNOS (Mouse)	nNOS (Rat)	eNOS (Bovine)
		a	S=	NI	NI	NI
23		b	Me-S-	23.9	2.0	6.8
	-CH_3	c	Et-S-	19.1	9.4	44.9
		d	Me-NH-	NI	NI	NI
24	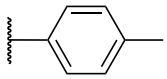	a	S=			
		b	Me-S-			
		c	Et-S-	All NI	All NI	All NI
		d	Me-NH-			
		e	Et-NH-			
25	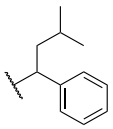	a	S=	NI	NI	
		b	Me-S-	NI	NI	
		c	Et-S-	31.0	NI	All NI
		d	Me-NH-	NI	NI	
		e	Et-NH-	NI	ND[b]	
26	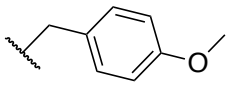	a	S=	NI		
		b	Me-S-	NI		
		c	Et-S-	22.9	All NI	All NI
		d	Me-NH-	NI		
		e	Et-NH-	NI		
27	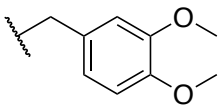	a	S=	NI	NI	
		b	Me-S-	NI	NI	
		c	Et-S-	39.5	19.6	All NI
		d	Me-NH-	NI	NI	
		e	Et-NH-	NI	NI	
28	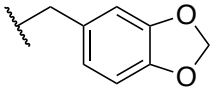	a	S=		NI	
		b	Me-S-		NI	
		c	Et-S-	All NI	45% at 100 μM	
		d	Me-NH-		NI	All NI
		e	Et-NH-		NI	
29	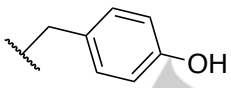	a	S=		NI	
		b	Me-S-		3.2	
		c	Et-S-	All NI	35.9	All NI
		d	Me-NH-		NI	
		e	Et-NH-		NI	
30	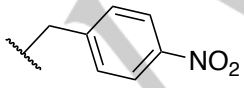	a	S=			
		b	Me-S-			
		c	Et-S-	All NI	All NI	All NI
		d	Me-NH-			
		e	Et-NH-			
31	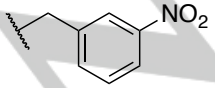	a	S=		NI	
		b	Me-S-		NI	
		c	Et-S-	All NI	34.2	All NI
		d	Me-NH-		ND	
		e	Et-NH-		NI	

[a]NI = no significant inhibition (<50% at 100 μM). [b]ND = not determined.

Table 3. Structures of 1,3,4-oxadiazoles **32**-**34** and *in vitro* NOS inhibition (IC_{50} in μM)[a]

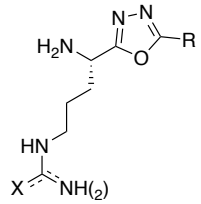

Cpds	R	Series	X	IC_{50} (μM) (or % inhibition at 100 μM)		
				iNOS (Mouse)	nNOS (Rat)	eNOS (Bovine)
32	-CH_3	a	S=	NI	NI	ND[b]
		b	Me-S-	NI	57.4	NI
		c	Et-S-	NI	NI	NI
		d	Me-NH-	NI	NI	NI
		e	Et-NH-	54.3	17.9	12.8
33	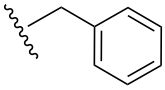	a	S=			
		c	Et-S-	All NI	All NI	All NI
		d	Me-NH-			
		e	Et-NH-			
34	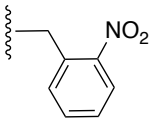	a	S=	NI	NI	
		b	Me-S-	NI	NI	
		c	Et-S-	7.2	26.9	All NI
		d	Me-NH-	NI	NI	
		e	Et-NH-	NI	NI	

[a]NI = no significant inhibition (<50% at 100 μM). [b]ND = not determined.

Table 4. Structures of 1,3,4-oxadiazoles **35**-**39** and *in vitro* NOS inhibition (IC_{50} in μM)[a]

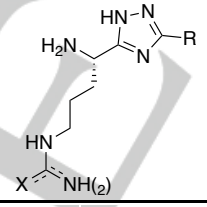

Cpds	R	Series	X	IC_{50} (μM) (or % inhibition at 100 μM)		
				iNOS (Mouse)	nNOS (Rat)	eNOS (Bovine)
35	-CH_3	a	S=	NI	NI	NI
		b	Me-S-	NI	NI	NI
		c	Et-S-	37.9	42.0	9.9
		d	Me-NH-	NI	NI	NI
		e	Et-NH-	NI	NI	NI
36	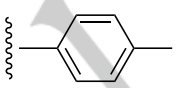	a	S=			
		b	Me-S-			
		c	Et-S-	All NI	All NI	All NI
		d	Me-NH-			
		e	Et-NH-			
37	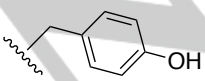	a	S=		NI	NI
		b	Me-S-		13.8	NI
		c	Et-S-	All NI	14.6	20.6
		d	Me-NH-		NI	NI
		e	Et-NH-		NI	NI
38	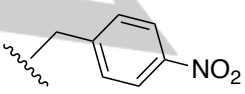	a	S=	NI	NI	
		b	Me-S-	45% at 100 μM	NI	
		c	Et-S-	14.5	16.1	All NI
		d	Me-NH-	NI	NI	
		e	Et-NH-	NI	NI	

39	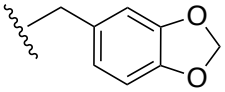	a b c d e	S= Me-S- Et-S- Me-NH- Et-NH-	All NI	All NI	All NI

[a]NI = no significant inhibition (<50% at 100 μM).

- *Stability of selected compounds in inhibition test conditions*. The chemical stability of a few *S*-alkyl-Itc compounds (dipeptide-like **11b** and **11c**, and 1,2,4-oxadiazole **31c**, all at 1 mM in 100 μM Hepes buffer, pH 7.5, at 30 °C) was checked alone or in the presence of 10 eq. benzylamine. Indeed, the *S*-alkyl-isothiourea could be converted into urea or react with nucleophiles (here yielding *N*-benzyl-guanidine in the presence of benzylamine). LC-MS analysis performed after 45 min and 3 h incubation showed no significant formation of urea or *N*-benzylguanidine (data not shown).

- *Spectral studies.* UV-Visible difference spectroscopy allows observation of interactions of substrates and inhibitors with the heme active site of NOS.[63] To better understand how some of the new compounds (dipeptide-like **7b**, **7c**, **19c**, **21c** and **22c**, 1,2,4-oxadiazoles **23b**, **23c**, **25c**, **26c**, and **31c**, 1,3,4-oxadiazole **34c**, 1,2,4-triazoles **35c** and **37c**) acted as inhibitors, we have studied their effects on the UV-visible spectra of the nNOS ($nNOS_{oxy}$) and iNOS ($iNOS_{oxy}$) oxygenase domains.[63] The UV–visible spectrum of $nNOS_{oxy}$ and $iNOS_{oxy}$ in Hepes buffer displayed a broad Soret peak with a maximum at 415 nm indicating that they predominantly existed as hexacoordinated heme–Fe^{III}–H_2O complexes, with water as the 6th axial ligand. When added to these proteins, L-arginine elicited difference spectra with a peak at ~395 nm and a trough at ~420 nm (type I interaction, data not shown). The stepwise additions of the selected compounds to n- and $iNOS_{oxy}$ gave in all cases rise to difference spectra characterized by a trough at ~425 nm and a peak at ~395 nm characteristic of type I interactions (Figure 2 for compound **23c**). These results showed that all the studied compounds bound in close proximity to the heme of n- and $iNOS_{oxy}$ and shifted the spin state equilibrium to the pentacoordinated heme–Fe^{III} state in a similar manner than the L-arginine substrate. Double reverse plotting of the differences in absorbance between peak at ~395 nm and valley at ~425 nm ($\Delta A_{395\text{-}425nm}$) as a function of the concentration of the added compounds allowed to calculate apparent binding constants (Ks) (Table 5). As a reference inhibitor, SEIT tightly bound both proteins with high affinity for $iNOS_{oxy}$ (Figure S5 in Supporting Information for SEIT). Surprisingly, compounds **7b-c** poorly bound both proteins. By contrast, dipeptide-like compounds **19c**, **21c** and **22c** preferentially bound $nNOS_{oxy}$ vs $iNOS_{oxy}$ with apparent affinities close to that of SEIT for this isoform. Similarly, 1,2,4-oxadiazoles **23b**, **23c**, **26c**, **31c**, 1,3,4-oxadiazole **34c** and 1,2,4-triazoles **35c** and **37c** preferentially bound $nNOS_{oxy}$ vs $iNOS_{oxy}$ but with lower affinity than the dipeptide-like compounds. Interestingly, in these series of compounds, similar selectivity of nNOS over iNOS was observed when comparing their inhibitory potencies (Tables 1-4). Only the 1,2,4-oxadiazole **25c** showed preference for $iNOS_{oxy}$ over $nNOS_{oxy}$ in accordance with its inhibitory potencies measured versus iNOS and nNOS (Table 2).

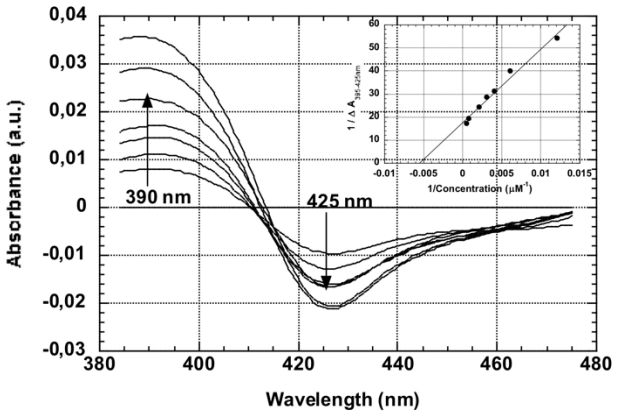

Figure 2. Difference spectrum obtained upon stepwise addition of increasing concentrations (from 7.5 μM to 2.0 mM) of **23c** to iNOSoxy in Hepes buffer, as described in Experimental section. Inset: plot of $1/(\Delta A_{395\text{-}425nm})$ vs 1/[**23c**].

Table 5. Apparent equilibrium constants (K_s, μM) for the binding of some dipeptides, 1,2,4-oxadiazoles, 1,3,4-oxadiazole and 1,2,4-triazoles to $nNOS_{oxy}$ and $iNOS_{oxy}$.[a]

Cpds	$nNOS_{oxy}$	$iNOS_{oxy}$
SEIT	6.4 ± 1.5	2.4 ± 0.4
Dipeptide-like		
7b	75 ± 9	56 ± 16
7c	122 ± 31	144 ± 56
19c	11.4 ± 3.8	50 ± 5
21c	9.6 ± 1.2	71 ± 10
22c	7.1 ± 2.6	406 ± 97
1,2,4-Oxadiazoles		
23b	37.4 ± 8.5	193 ± 36
23c	164 ± 25	178 ± 19
25c	253 ± 129	69 ± 13
26c	311 ± 59	351 ± 56
31c	40 ± 13	162 ± 21
1,3,4-Oxadiazole		
34c	68 ± 8	> 500
1,2,4-Triazoles		
35c	166 ± 19	487 ± 51
37c	163 ± 42	311 ± 141

[a] Titrations were performed by UV/Vis difference spectroscopy as described in Experimental Section. Values ± SD from three different experiments.

- *Inhibition of NOS in cells.* To study the potential of these compounds to inhibit NOS expressed in cells, we performed

several experiments with the two more potent compounds, the dipeptide-like **7b** and the 1,2,4-oxadiazole **23c**. L-N^6-(1-iminoethyl)-lysine (L-NIL)[31] and/or *S*-ethyl isothiourea (SEIT),[64] two well-known potent and quite selective iNOS inhibitors were used as positive controls.

First, cell viability was evaluated in the murine macrophage RAW 264.7 cells using a MTT assay. This experiment was performed with 1 µg/mL or without LPS, which induces iNOS expression. In the absence of LPS, none of the compounds tested modified cell viability. In the presence of LPS (1 µg/ml), cell viability was reduced by 42% due to the inhibition of key enzymes involved in cell metabolism (e.g. cytochrome oxidase) by NO.[65] L-NIL and SEIT partially reversed this effect by respectively 26% and 32% at 100 µM (P<0.05, n = 6) (Figure 3A and 3B). Cell viability was also improved by 18% and 22% for compounds **7b** (P<0.05, n = 6) (Figure 3C) and **23c** (P<0.05, n = 6) (Figure 3D), respectively, at the same concentration. These results indicated that **7b** and **23c** could at least partially reverse the iNOS-derived toxicity of NO and had significant ability to enter the cells.

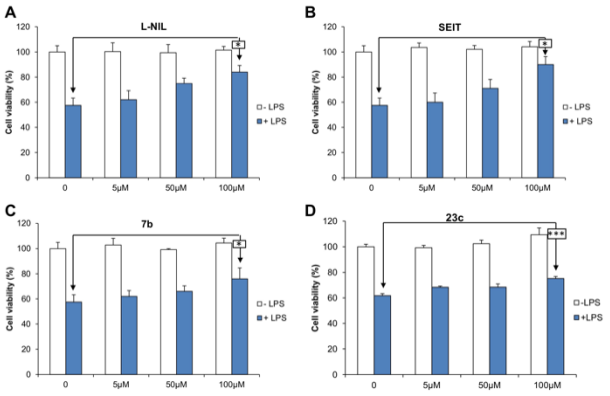

Figure 3. Effects of L-NIL, SEIT, **7b** and **23c** on cell viability: MTT assay on RAW 264.7 in the presence or not of LPS (1µg/mL). *, P<0.05; ***, P<0,001.

Then, we evaluated their ability to inhibit iNOS in RAW 264.7 cells (Figure 4) and in the rat pancreatic β-cell line INS-1 (Figure 5), where iNOS was induced by LPS (1 µg/mL) or IL-1β (1 ng/mL), respectively.

Nitrite accumulation in the supernatant of RAW 264.7 cells in the presence of LPS was used as a measurement of iNOS activity. We observed a dose-dependent decrease in NO production with increasing concentrations of L-NIL and SEIT, reaching respectively -66% and -75 % at 100 µM (*P*<0.001, *n*=4) (Figure 4). The two compounds were already active at a 5 µM concentration (L-NIL, P<0.001; SEIT, P<0.01). Compound **7b** also reduced NO production starting at 10 µM (P<0.01) and with a maximum of -61% at 100 µM (*P*<0.001, *n*=8) (Figure 4). Compound **23c** decreased NO production to a lesser extent (-32% at 100 µM; *P*<0.001, n = 4), with a detectable effect at 50 µM (P<0.01) (Figure 4). No compound induced noticeable cell toxicity.

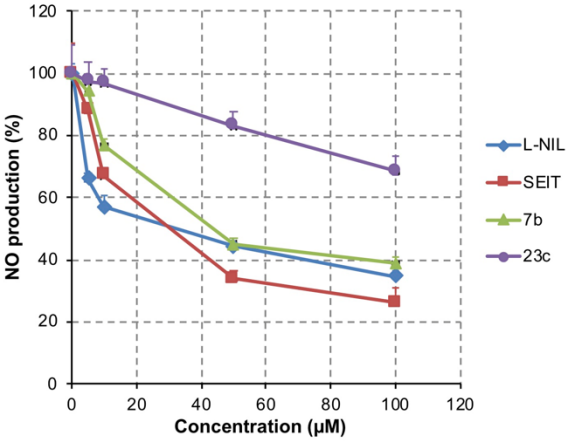

Figure 4. Inhibitory effects of L-NIL, SEIT and compounds **7b** and **23c** on NO production by RAW 264.7 cells stimulated by LPS (1µg/mL).

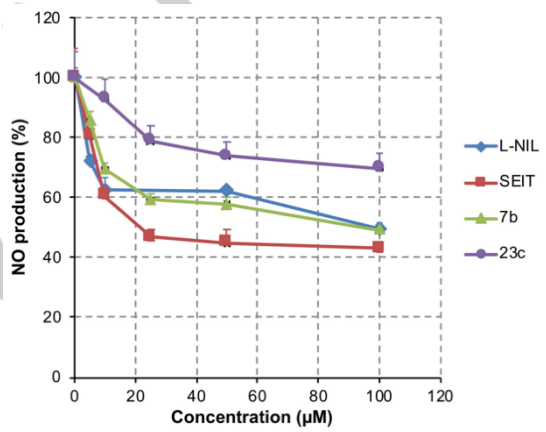

Figure 5. Inhibitory effects of L-NIL, SEIT and compounds **7b** and **23c** on NO production by INS-1 cells stimulated by IL-1β (1 ng/mL).

In INS-1 cells, L-NIL and SEIT reduced NO production by respectively 51% (*P*<0.001, *n*=4) and 77% (*P*<0.01, n = 4) at 100 µM (Figure 5). Compound **7b** showed an effect comparable to that of L-NIL (-51% at 100 µM; *P*<0.001, *n*=8) (Figure 5). All three compounds started to be active at 5 µM concentration (L-NIL, P<0.01; SEIT, P<0.05; **7b**, P<0.001). Compound **23c** was less potent than **7b** with a noticeable inhibitory activity at 25 µM (P<0.05), but of equal efficiency in the two cell lines (-30% at 100 µM; P<0.05, n = 4) (Figure 5). The 1,3,4-oxadiazole **34c** and the 1,2,4-triazole **35c** were also evaluated in the same experimental conditions. They were inactive with no effect on NO production in RAW 264.7 cells (data not shown) probably due to lack of membrane permeability.

Finally, we assessed the ability of the compounds to restore insulin secretion after induction of iNOS. Indeed, when iNOS is induced in INS-1 cells, insulin secretion induced by basal (2.8 mM) and stimulating (5.6 mM) glucose was reduced by respectively 42 and 55% (Figure 6A). L-NIL partially improved insulin secretion in the presence of 5.6 mM glucose with a maximum effect at 25 µM concentration. Compound **7b** also restored insulin secretion in the presence of 5.6 mM glucose at 10 and 25 µM (*P*<0.05, *n*=5) (Figure 6B). These results are

of interest as iNOS inhibition was found to protect beta cells against the deleterious effects of pro-inflammatory cytokines, which in type 1 diabetes are a major cause of beta-cell destruction.[66,67]

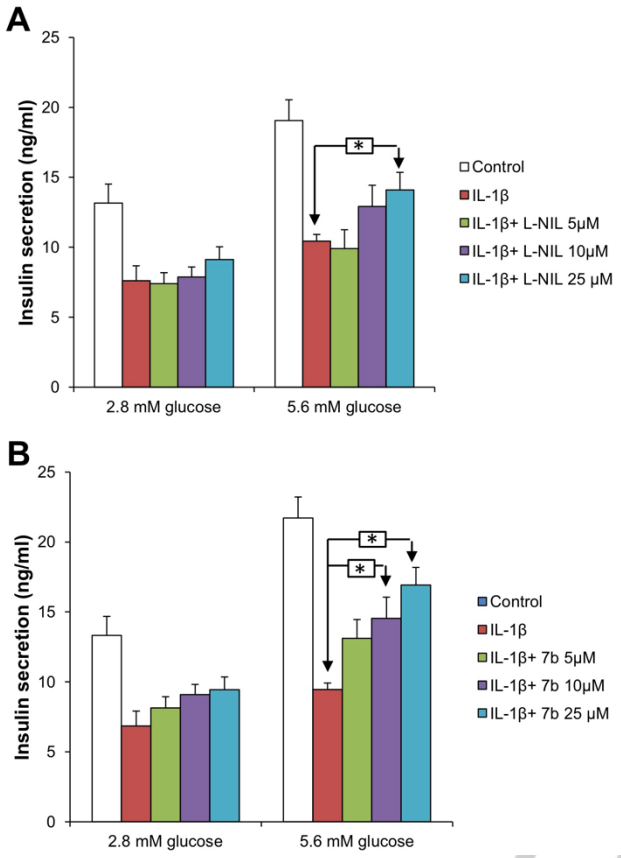

Figure 6. Effect of L-NIL (A) and compound **7b** (B) on insulin secretion by INS-1 cells in the presence of 2.8 (basal) or 5.6 mM glucose and after iNOS induction with IL-1β (1 ng/mL). *, P<0.05.

Overall, these results support that compound **7b** was able to inhibit intracellular iNOS and to affect cellular functions.

Conclusion

In this study, we have synthesized 164 compounds (5 amino acids, 76 dipeptide-like compounds, 44 1,2,4-oxadiazoles, 14 1,3,4-oxadiazoles, and 25 1,2,4-triazoles) using an original solid-phase synthetic strategy. This straightforward synthetic strategy was implemented with generally efficient and simple reactions, allowing the rapid preparation of numerous compounds with satisfying crude purity. Beside the synthesis on PS resin, we have prepared two libraries of dipeptide-like and 1,2,4-oxadiazole analogues on Lantern supports. This approach has great potential for the combinatorial synthesis of many more analogues from the lead compounds discovered in this study.

All compounds were tested against three recombinant NOS isoforms. Overall, several new compounds showed significant inhibitory activity (IC_{50} about 2 to 80 μM) toward at least one NOS, with a global preference for nNOS, followed by iNOS, whereas eNOS was scarcely inhibited. These results are in accordance with Silverman's team studies on nitro-arginine-containing dipeptides, which were shown to be highly selective against eNOS. The observed main preference for the *S*-Et-Itc analogues could be related to the study about a series of *S*-alkylisothiourea developed as non-selective NOS inhibitors, where SEIT was found to be the best inhibitor.[68] These results, supported by the X-ray structure of hiNOS-SEIT complex,[23] suggested that the *S*-ethyl moiety was optimal for binding. While some dipeptide-like compounds were found significantly active as expected from previous studies,[26,50] it is noteworthy that active compounds were also identified in the not yet described dipeptide mimetic series containing various five-membered-heterocycles. This is an important finding as these heterocyclic compounds are expected to be more stable and less flexible than the dipeptide-like analogues. Our results open the way to the development of new heterocyclic compounds only containing a *S*-Et-Itc derivative as a substrate analogue that could take advantage of differences along the substrate access channel for NOS isoform selectivity.

Experimental Section

- Chemistry

- *General.* Protected amino acids, BOP, DIEA, TFA, piperidine, solvents and other reagents were purchased from Iris-Biotech, Novabiochem, Riedel-de Haën, Carlo Erba or Acros organics and used without further purification. Fmoc Rink amide polystyrene resin (100-200 mesh, 0.94 mmol/g) and Synphase lanterns (35 μmol loading) were purchased from Iris-Biotech and Mimotopes, respectively. Solvents used for RP-HPLC and LC-MS were of HPLC grade. Amidoximes were either commercially available or have been synthesized as previously described.[56]

- *NMR and IR spectroscopy.* ^{1}H NMR spectra were recorded at 300, 400 or 500 MHz using DMSO-d_6 or $CDCl_3$ solutions. Splitting patterns are designated as follows: s, singlet; d, doublet; t, triplet; q, quartet; m, multiplet; br, broad. ^{13}C NMR spectra were recorded at 75, 101 or 125 MHz using DMSO-*d6* solutions.

IR spectra were collected on a Perkin Elmer Spectrum One apparatus.

- *Analysis and purification.* Thin-layer chromatography was performed on aluminium backed sheets of silica gel F_{254} (0.2 mm), which were visualized under 254 nm light and by spraying with a 2% EtOH solution of ninhydrin followed by heating, or by charring with an aqueous solution of ammonium sulfate and sulfuric acid (200 g $(NH_4)_2SO_4$ and 40 mL concentrated sulfuric acid in 1 L of water).

RP-HPLC analysis was performed using the following conditions: Chromolith SpeedRod C18 column (0.46 x 5 cm), linear gradient (0-100%) of eluent B in A over 5 min (flow rate: 3 mL/min). Eluent A: 0.1% aqueous TFA; eluent B: acetonitrile/0.1% TFA. Detection was made at 214 nm.

Purification by preparative RP-HPLC was performed on a Waters Delta Pak C18 column (40 x 100 mm, 15 μm, 100 Å), linear gradient of eluent B in A at a 1%/min rate (flow rate: 28 mL/min). Eluent A: 0.1% aqueous TFA; eluent B: acetonitrile/0.1% TFA. In the case of the libraries of dipeptide-like and 1,2,4-oxadiazole compounds, their purification was performed on a reverse-phase preparative HPLC

coupled to mass spectrometer (Autopurif system from Waters driven by the software MassLynx 4.0 Fractonlynx) using a Waters X Bridge Prep C18 column (19 x 100 mm, 5 μm) and a linear gradient of eluent B in A (flow rate: 20 mL/min).

Column chromatography was performed using Merck silica gel 60 of particle size 40-63 μm.

Mass spectrometry: samples were prepared in acetonitrile/water (50/50 v/v) mixture. The LC-MS system consisted of a Waters Alliance 2690 HPLC, coupled to a Waters-Micromass ZQ spectrometer (electrospray ionization mode, ESI+). All analyses were carried out using a RP C18 monolithic Onyx Phenomenex column (25 x 4.6 mm), linear gradient (0–100%) of eluent B in A over 3 min (flow rate: 3 mL/min). Eluent A: 0.1% aqueous formic acid; eluent B: acetonitrile/0.1% formic acid. Positive ion electrospray mass spectra were acquired at a solvent flow rate of 100–500 μL/min. Nitrogen was used as both the nebulizing and drying gas. The data were obtained in a scan mode in 0.1 s intervals; 10 scans were summed up to get the final spectrum.

HR-MS were registered on a JEOL JMS-SX-102A mass spectrometer.

The HPLC retention times, calculated monoisotopic mass and measured high resolution mass of the compounds, NMR data and yields of purified products are reported in Supporting Information

Synthesis of resin supported intermediates 4, 5 and 6.

- Boc-Orn(Z)-OMe, **1**. To a solution of Boc-Orn(Z)-OH (25 g, 68.2 mmol) in DMF were added Na_2CO_3 (14.46 g, 136 mmol) and MeI (8.07 mL, 129.6 mmol). After 5 h stirring at room temperature, the reaction mixture was filtered and concentrated. The residue was taken up in AcOEt (100 mL) and the organic phase was washed with water, aqueous 1 M $KHSO_4$, water, saturated aqueous $NaHCO_3$, water and saturated aqueous NaCl, dried over $MgSO_4$ and concentrated *in vacuo* to give a yellow solid (25.8 g, 99%), which was used without further purification. R_f 0.45 (AcOEt/hexane, 3:7); t_R 2.69 min; *m/z* (ES+) 381.3 $[M + H]^+$, 325.3 $[M – tBu + H]^+$, 281.3 $[M –Boc +H]^+$. ^{1}H NMR (300 MHz, DMSO-d_6) δ 1.38 (s, 9H), 1.45-1.64 (m, 4H), 2.97 (m, 2H), 3.61 (s, 3H), 3.94 (m, 1H), 5.00 (s, 2H), 7.24 (m, 2H), 7.34 (m, 5H); ^{13}C NMR (75 MHz, DMSO-d_6) δ 26.0, 28.0, 28.2, 40.2, 51.7, 53.3, 65.1, 78.2, 127.7, 128.3, 137.3, 155.5, 156.1, 173.1.

- Boc-Orn-OMe, TFA salt, **2**. To a solution of **1** (25.8 g, 67.9 mmol) in ethanol, was added slowly and under strong stirring TFA (7.6 mL, 102 mmol), followed by 4 g of 10% Pd/C. After 4 h stirring at room temperature under H_2 bubbling, the suspension was filtered on celite and the filtrate was evaporated to give a white solid (24.4 g, 100%). t_R 1.50 min; *m/z* (ES+) 247.2 $[M + H]^+$, 191.2 $[M – tBu + H]^+$, 147.2 $[M – Boc +H]^+$. ^{1}H NMR (300 MHz, DMSO-d_6) δ 1.38 (s, 9H), 1.55-1.75 (m, 4H), 2.76 (m, 2H), 3.62 (s, 3H), 3.95 (m, 1H), 7.29 (d, *J* = 7.56 Hz, 1H), 7.82 (s, 3H); ^{13}C NMR (75 MHz, DMSO-d_6) δ 24.5, 28.2, 28.8, 39.0, 52.4, 53.6, 78.9, 156.2, 173.5.

- Methyl *Nα*-(*tert*butoxycarbonyl)-*Nδ*-(thioxomethylene)-*L*-ornithinate (Boc-L-Orn(Nδ=C=S)-OMe), **3**. To a solution of **2** (24.4 g, 67.8 mmol) in THF (250 mL) were added at 0°C under strong stirring CS_2 (36.2 mL, 0.6 mol) immediately followed by TEA (32.6 mL, 232 mmol). The reaction was stirred for 45 min at this temperature and 81 mL (0.9 mol) of H_2O_2 were added dropwise. The mixture was then diluted with diethylether (725 mL). The organic layer was washed with aqueous 1 M $KHSO_4$, water, saturated aqueous $NaHCO_3$, water and saturated aqueous NaCl, dried over $MgSO_4$ and concentrated *in vacuo* to afford after chromatographic purification over silica gel (hexane/AcOEt (5:1)) a yellowish oil (14 g, 72%). R_f 0.26 (AcOEt/hexane, 1:5); t_R 2.77 min; *m/z* (ES+) 289.1 $[M + H]^+$, 233.1 $[M – tBu + H]^+$, 189.1 $[M –Boc +H]^+$; IR ν_{max} cm^{-1} 3373, 2977, 2926, 2182, 2096, 1742, 1704; ^{1}H NMR (300 MHz, DMSO-d_6) δ 1.38 (s, 9H), 1.65-1.75 (m, 4H), 3.63 (s, 3H), 3.64-3.68 (m, 2H), 4.00 (m, 1H), 7.34 (d, *J* = 7.56 Hz, 1H); ^{13}C NMR (75 MHz, DMSO-d_6) δ 25.9, 27.8, 28.1, 44.4, 51.8, 52.8, 78.3, 127.3, 155.5, 172.8.

- Boc-Tci(*Nω*-Rink amide)-OMe, **4**. A portion of Fmoc-protected Rink amide resin (0.94 mmol/g substitution) was loaded in a peptide synthesis reaction vessel and swelled in DMF for 15 min. The resin was then treated twice (5 min + 20 min) with a solution of 20% piperidine in DMF to remove the Fmoc-protecting group, washed with DMF, DCM, MeOH, and dried under vacuum. The deprotected peptide-resin was placed in a balloon and swelled in dry THF for 15 min and a solution of compound **3** (3 equiv.) and TEA (3.1 equiv.) in THF (10 mL per g of resin) was added. The suspension was stirred at 65 °C for 3 h and at room temperature overnight. Completion of the reaction was assessed using the TNBS test (see below). The resin was finally filtered, washed with THF and DCM and dried.

In the case of Fmoc-Rink amide-loaded Synphase lanterns (35 μmol per unit), they were first labelled with color-coded tagging using stems and cogs of different colors. Then, they were introduced in drilled-capped glass bottles and conditioned in DMF. After removal of solvent, a solution of 20% piperidine in DMF to remove the Fmoc-protecting group was added to cover all lanterns. After 20 min without stirring, the treatment was repeated for the same duration and the lanterns were washed with DMF (3 x 3 min), MeOH (3 x 3 min) and DCM (3 x 3 min) and dried. Loading of compound **3** was performed in the same conditions as described above, taking care that lanterns are covered with solvent. Lanterns were finally washed with DMF, MeOH and DCM (3 x 3 min each solvent) and dried. A small piece of one lantern was cut to check reaction completion with the TNBS test.

- Boc-Tci(*Nω*-Rink amide)-OH, **5.** Saponification of **4** was performed according to Cantel S. et al..[53] A portion of the resin **4** was loaded in a peptide synthesis reaction vessel and swelled in THF for 15 min. A 2 M aqueous solution of LiOH (5 equiv.) was then added. Volumes were calculated on the basis of a 7/3 THF/H_2O ratio. After 15 h stirring at room temperature, the resin was washed with THF, DCM and MeOH, and dried. Completion of the reaction was assessed by LC-MS analysis after a cleavage test (see below).

For Synphase lanterns, saponification was similarly carried out but without stirring and respecting 3 x 3 min duration for each solvent washing.

- Boc-Tci(*Nω*-Rink amide)-$NHNH_2$, **6.** A portion of the resin **4** was loaded in a peptide synthesis reaction vessel and swelled in THF for 15 min. Hydrazine hydrate (5 equiv.) was then added and the mixture was stirred at room temperature for 24 h. The resin was washed with DMF, DCM and MeOH, and dried. Completion of the reaction was assessed by LC-MS analysis after a cleavage test (see below). A TNBS test gave dark red resin beads, due to the hydrazide amine group.

General procedures for synthesis.

A) Synthesis of supported dipeptide-like ***7-22****.* A portion of the supported thiocitrulline intermediate **5** was swelled in DMF or NMP for 15 min and filtered. Were then successively added DMF or NMP solutions of amine compound (1.3 equiv.), HOAt (1.3 equiv.), DIEA (1.5 equiv.) and BOP (1.3 equiv.). After 12 h stirring, the resin was filtered and washed with DMF and the coupling was repeated. The resin was finally washed with DMF and DCM and dried.

In the case of Synphase lanterns, the same conditions were followed and final volume of DMF or NMP was 10 mL/10 lanterns.

B) Synthesis of supported 1,2,4-oxadiazole derivatives ***23-31****.* This procedure was adapted from a solution protocol described by Hamzé et al.[56] and was composed of a coupling step followed by a cyclo dehydration step. A portion of the supported thiocitrulline intermediate **5** was placed in a balloon, swelled in DMF/DCM (9:1) for 15 min and cooled to –10°C. Were then added the amidoxime derivative (1.2 equiv.), HOBt (1.2 equiv.) and DIC (1.2 equiv.). After 20 min at –10°C and 4 h at room temperature, the resin was filtered and washed with DMF and the coupling was repeated. The resin was finally washed with DMF, DCM and MeOH. For the cyclo dehydration step, it was conditioned in THF/H_2O (7:3). Sodium acetate (1.1 equiv.) was then added and the mixture was refluxed during 5 h. The resin was finally washed with DMF, DCM and MeOH, and dried.

In the case of Synphase lanterns, the same conditions were followed and final volume of DMF/DCM or THF/H_2O was 10 mL/10 lanterns.

C) Synthesis of supported 1,3,4-oxadiazole derivatives ***32-34****.* This procedure was adapted from James et al.[57] and was composed of a coupling step followed by a cyclo dehydration step. A portion of the supported thiocitrulline intermediate **6** was swelled in DMF for 15 min and DIEA (4 equiv.), a carboxylic compound (3 equiv.) and HBTU (3 equiv.) were added. After 4 h stirring at room temperature, the resin was filtered and washed with DMF, MeOH and DCM. Completion of the coupling step was assessed by the TNBS test. In case of positive test, the coupling step was repeated. For the cyclodehydration step, the dried resin was swelled in dry acetonitrile and DIEA 10 equiv.) and C_2Cl_6 (2.6 equiv.) were added, followed, after 5 min, by PPh_3 (4 equiv.). After 30 min stirring at room temperature, the resin was washed with DMF, DCM and MeOH and dried.

D) Synthesis of supported di-substituted 1,2,4-triazole derivatives ***35-39****.* A portion of the supported thiocitrulline intermediate **6** was placed in a balloon and swelled in 2-methoxyethanol for 15 min. An amidine or amidoxime derivative (5 equiv.) was then added and the reaction mixture was stirred under reflux for 24 h. The resin was finally washed with DMF, DCM and MeOH, and dried.

E) Synthesis of supported S-Methyl-isothiourea derivatives. A supported thiourea derivative was swelled in DMF for 15 min, filtered and a 0.2 M solution of MeI (15 equiv.) in DMF was added. The reaction was stirred at room temperature for 1 h and was repeated twice. The resin was then washed with DMF and DCM and dried.

*F) Synthesis of supported S-Ethyl-isothiourea derivatives. S-*Ethylation of thiourea compounds was performed as *S*-methylation but in a balloon at 45°C and in the presence of a 0.4 M solution of EtI (30 equiv.) in DMF.

G) Synthesis of supported N-Methyl-guanidine derivatives. A supported *S*-methyl-isothiourea derivative was treated with a 2 M solution of $MeNH_2$, HCl (60 equiv.) and NMM (60 equiv.) in dry DMSO in a sealed vessel resistant to pressure. The suspension was stirred at 80°C for 14 h, cooled and the resin was washed with water, MeOH and DCM, and dried.

H) Synthesis of supported N-Ethyl-guanidine derivatives. A supported *S*-methyl-isothiourea derivative was treated with a 2.5 M solution of $EtNH_2$, HCl (75 equiv.) and NMM (75 equiv.) in dry DMSO in a sealed vessel resistant to pressure. The suspension was stirred at 80°C for 14 h, cooled and the resin was washed with water, MeOH and DCM, and dried.

I) Cleavage from the solid support.

- Final cleavage of compounds from the solid support was performed with TFA/TIS/H_2O (95:2.5:2.5, 10 mL/g resin) at room temperature for 2 h with the exception of *S*-methyl and *S*-ethyl isothiourea analogues, which were submitted to the cleavage mixture for 3h at 30 °C. After resin filtration, the filtrate was concentrated under vacuum, and compounds were precipitated by diethyl ether addition and recovered after centrifugation. The pellet was washed twice with diethyl ether. When no precipitation occurred, the residues were solubilized in water/MeCN (50:50) and freeze-dried. All compounds were obtained with an average yield of 5%-80% after reverse-phase HPLC purification. All compounds were above 90-95% purity.

- Cleavage test: some reaction steps (loading of compound **3** onto the solid support and its saponification, *S*-ethylation and guanidinylation for selected compounds) were checked by cleaving 2-3 mg of resin with a solution of TFA/TIS/H_2O (95:2.5:2.5, v/v/v, 0.5 mL) for 30 min at room temperature. After filtration, the mixture was evaporated under a nitrogen stream and the residue was precipitated with diethylether. Precipitate was collected by filtration, solubilized in 50% MeCN/H_2O and submitted to LCMS analysis.

J) TNBS test. An aliquot portion of resin beads or a small piece of one lantern is collected and treated with one drop of a 1 M TNBS solution in DMF and one drop of a 10% DIEA solution in DMF (v/v). Colourless support after 1 min at room temperature indicates the absence of free amine groups. The presence of free amine groups gives a red colour. In the case of the hydrazide resin **6**, the free NH_2 gives a dark brown colour.

- Biological evaluation.

L-Arginine, L-citrulline, *Nω*-nitro-L-arginine, dithiothreitol (DTT), hemoglobin, superoxide dismutase, catalase, bovine serum albumin, L-NIL, SEIT, (*6R*)-5,6,7,8-tetrahydrobiopterin, NADPH, porcine brain calmodulin and all common salts and buffers were purchased from Sigma-Aldrich.

A) *Production of recombinant NOSs*. Full length recombinant rat nNOS, mouse iNOS, bovine eNOS, and the heme domains of rat brain nNOS and mouse iNOS were expressed in *Escherichia coli* and purified as described previously.[69-73] Protein concentrations were determined by the method of Bradford using bovine serum albumin as a standard and the Bradford reagent from Biorad.[74] The heme concentrations of the purified NOS were determined optically from the [Fe^{II}-CO] – [Fe^{II}] difference spectrum using a $\Delta\varepsilon_{445\text{-}480nm}$ of 74 $mM^{-1}.cm^{-1}$.[75] They were estimated to be more than 95% pure by SDS-PAGE electrophoresis.

B) *Measurement of NO production by recombinant NOSs.* NOS catalytic activity was measured using the hemoglobin capture assay.[59] The test was performed at 30 °C in 96-well microplates using a final volume of 200 µl. The assay mixture contained 100 µM NADPH, 10 µM BH_4, 6 µM HbO_2, 100 µM DTT, 5 µM FAD, 5 µM FMN, 10 µM (nNOS and eNOS) or 20 µM (iNOS) arginine, all in 100 mM Hepes buffer, pH 7.5, and, for constitutive n- and e-NOS, 10 µg/mL calmodulin and 1 mM $CaCl_2$. The studied compounds were introduced as 2 µL of x100 concentrated solutions in DMSO and control experiments were performed with DMSO or buffer only. The kinetics of NO production was measured at 401 nm using the Infinite F500 microplate reader (Tecan).

C) Effects of selected compounds on UV-visible spectra of n- and iNOSoxy. Optical spectra were recorded using an Uvikon 941 spectrophotometer in 150 µL quartz cuvettes. The apparent binding affinities of the studied compounds with the n- and iNOSoxy active sites were determined by perturbation difference spectroscopy at room temperature.[63] The native enzymes (~1 µM in 50 mM Hepes buffer, pH 7.4) were equally divided into reference and sample cuvettes and a baseline was recorded. Increasing concentrations (usually in the 1 µM – 1 mM range) of the studied compounds in

buffer (or DMSO) were added to the sample cuvette and equivalent amounts of buffer (or DMSO) were added to the reference cuvette. Apparent dissociation constants ($K_{s\ app}$) were estimated by plotting the difference in absorbance between peak (~395 nm) and valley (~425 nm) versus concentration of the added compound as a double reciprocal plot. Linear fittings of the data were performed by KaleidaGraph (Version 4.1, Synergy Software).

D) *Evaluation on cellular models.* The macrophage cell line RAW 264.7 (a gift from Dr A. Blangy, Montpellier, France) was cultured in Dulbecco's Modified Eagle's Medium (DMEM), supplemented with 10% FCS, 100 units/mL penicillin, 100 µg/mL streptomycin and 2 mM L-glutamine.

The insulin-secreting cell line INS-1 (a gift from Prof. C. Wolheim, Geneva, Switzerland) was cultured in RPMI-1640 supplemented with 10% FCS, 100 units/ml penicillin, 100 µg/mL streptomycin, 2 mM L-glutamine, 10 mM HEPES, 1 mM sodium pyruvate and 50 mM 2-mercaptoethanol, according to the method of M. Asfari et al.[76]

In RAW 264.7 cells, iNOS was induced by LPS (1µg/mL, Sigma Aldrich) during 24h, and, in INS-1 cells, by IL-1β (1 ng/mL) during 48h. All studied compounds were incubated with cells during the last 24h. *S*-ethylisothiourea (SEIT) and *L*-NIL were used as positive controls (Sigma Aldrich).

Cellular NO production was measured using Griess reagent (Sigma Aldrich), which evaluates the nitrite content in culture media.[77] Cellular toxicity was estimated by the MTT assay (Sigma Aldrich) in RAW 264.7 cells after induction (or not) of iNOS by LPS, according to the manufacturer's recommendations.

The functional effects of L-NIL and compound **7b** was evaluated on INS-1 cells. After incubation with the compounds during the last 24h of iNOS induction, cells were preincubated for 1 h at 37°C in Krebs-Ringer bicarbonate buffer (108 mM NaCl, 1.19 mM KH_2PO_4, 4.74 mM KCl, 2.54 mM $CaCl_2$, 1.19 mM $MgSO_4.7H_2O$, and 18 mM $NaHCO_3$), containing 2 g/L BSA in the absence of glucose. After removal of the medium, the cells were incubated for another hour at 37°C in the same buffer in the presence of basal (2.8 mM) and 5.6 mM glucose. At the end of the incubation period, the medium was collected and insulin measured using insulin high range assay kit (CisBio, Codolet, France).

Data are expressed as means ± SEM of n experiments (indicated in the result part).

Abbreviations

Boc, *tert*-butyloxycarbonyl; *BOP*, (benzotriazol-1-yloxy)tris(dimethylamino)phosphonium, hexafluorophosphate; *DCM*, dichloromethane; *DIC*, diisopropylcarbodiimide; *DIEA*, diisopropylethylamine; *DMF*, dimethylformamide; *DMSO*, dimethylsulfoxide; *ESI-MS*, electron spray ionization mass spectrometry; *HBTU*, *N*-[(1*H*-benzotriazol-1-yloxy) (dimethylamino)methylene]-*N*-methylmethanaminium hexafluorophosphate; *Hepes*, 4-(2-hydroxyethyl)-1-piperazine-ethanesulfonic acid; *HPLC*, high performance liquid chromatography; *HOBt*, hydroxybenzotriazole; *HRMS*, high resolution mass spectrometry; *IL-1β*, interleukin-1β; *Itc*, isothiocitrulline ; *LC-MS*, liquid chromatography coupled to mass spectrometry; *L-NIL*, L-*N*$^{\square}$-(1-iminoethyl)-lysine; *LPS*, lipopolysaccharide; *MTT*, 3-(4,5-dimethylthiazol-2-yl)-2,5-diphenyltetrazolium bromide; *NMM*, *N*-methyl-morpholine; *NMP*, *N*-methyl pyrrolidone; *NOHA*, N^{ω}-hydroxy-L-arginine; *n, i and eNOS*, neuronal, inducible and endothelial nitric oxide synthase, respectively; *Pip*, piperidine; *PS*, polystyrene; *HPLC*, high performance liquid chromatography; *rt*, room temperature; R*t*, retention time; *SEIT*, *S*-ethyl-isothiourea; t*Bu*, *tert*-butyl; *Tci*, thiocitrulline ; *TEA*, triethylamine; *TFA*, trifluoroacetic acid; *THF*, tetrahydrofuran; *TIS*, triisopropylsilane; *TNBS*, 2,4,6-trinitrobenzene-1-sulfonic acid; *Z*, benzyloxycarbonyl.

Acknowledgements

T.T. was supported by the Fondation pour la Recherche Médicale (DCM20121225755). The authors thank D^{r} D. J. Stuehr (Cleveland Clinic Fundation, Cleveland, USA) for providing NOS isozymes plasmids, and Pierre Sanchez for performing mass spectrometry analyses.

Conflict of Interest

The authors declare no conflict of interest.

Keywords: arginine • heterocycles • NO synthases inhibitors • solid phase synthesis • thiocitrulline

[1] D. S. Bredt, S. H. Snyder, *Annu. Rev. Biochem.* **1994**, *63*, 175-195.
[2] W. K. Alderton, C. E. Cooper, R. G. Knowles, *Biochem. J.* **2001**, *357*, 593-615.
[3] A.-D. Lajoix, H. Reggio, T. Chardès, S. Péraldi-Roux, F. Tribillac, M. Roye, S. Dietz, C. Broca, M. Manteghetti, G. Ribes, C.B. Wolheim, R. Gross, *Diabetes* **2001**, *50*, 1311-1323.
[4] C. Bogdan, *Trends Immunol.* **2015**, *36*, 161-178.
[5] D. J. Stuehr, *Biochim. Biophys. Acta* **1999**, *1411*, 217-230.
[6] S. Daff, *Nitric Oxide* **2010**, *123*, 1-11.
[7] D. J. Stuehr, M. M. Haque, *Br. J. Pharmacol.* **2019**, *176*, 177-188.
[8] P. Vallance, *Fundam. Clin. Pharmacol.* **2003**, *17*, 1-10.
[9] M.A. Carvalho-Filho, M. Ueno, S.M. Hirabara, A.B. Seabra, J.B. Carvalheira, M.G. de Oliveira, L.A. Velloso, R. Curi, M.J. Saad, *Diabetes* **2005**, *54*, 959-967.
[10] M. C. Franco, A. G. Estévez, *Cell. Mol. Life Sci.* **2014**, *71*, 3939-3950.
[11] N. T. Moldogazieva, S. V. Lutsenko, A. A. Terentiev, *Cancer Res.* **2018**, *78*, 6040-6047.
[12] G. Ferrer-Sueta, N. Campolo, M. Trujillo, S. Bartesaghi, S. Carballal, N. Romero, B. Alvarez, R. Radi, *Chem. Rev.* **2018**, *118*, 1338-1408.
[13] N. R. Sims, M. F. Anderson, *Neurochem. Int.* **2002**, *40*, 511-526.
[14] V. L. Dawson, T. M. Dawson, *Prog. Brain Res.* **1998**, *118*, 215-229.
[15] A. Boveris, S. Alvarez, A. Navarro, *Free Radic. Biol. Med.* **2002**, *33*, 1186-1193.
[16] M. Perreault, A. Marette, *Nat. Med.* **2001**, *7*, 1138-1143.
[17] S. Mocellin, V. Bronte, D. Nitti, *Med. Res. Rev.* **2007**, *27*, 317-352.
[18] E. A. Grimm, J. Ellerhorst, C. H. Tang, S. Ekmekcioglu, *Nitric Oxide* **2008**, *19*, 133-137.
[19] J. Li, C. V. Vause, P. L. Durham, *Brain Res.* **2008**, *1196*, 22-32.
[20] M. A. Cinelli, H. T. Do, G. P. Miley, R. B. Silverman, *Med. Res. Rev.* **2019**, doi: 10.1002/med.21599.
[21] P. Vallance, J. Leiper, *Nat. Rev. Drugs Discov.* **2002**, *1*, 939-950.
[22] B. R. Crane, A. S. Arvai, D. K. Ghosh, C. Wu, E. D. Getzoff, D. J. Stuehr, J. A. Tainer, *Science* **1998**, *279*, 2121-2126.
[23] T. O. Fischmann, A. Hruza, X. D. Niu, J. D. Fossetta, C. A. Lunn, E. Dolphin, A. J. Prongay, P. Reichert, D. J. Lundell, S. K. Narula, P. C. Weber, *Nat. Struct. Biol.* **1999**, *6*, 233-242.
[24] T. Doukov, H. Li, T. L. Poulos, *Biochemistry* **2009**, *48*, 10246-10254.
[25] H. Li, J. Jamal, C. Plaza, S. H. Pineda, G. Chreifi, Q. Jing, M. A. Cinelli, R. B. Silverman, T. L. Poulos, *Acta Cryst. D Biol. Cryst.* **2014**, *D70*, 2667-2674.
[26] R. B. Silverman, *Acc. Chem. Res.* **2009**, *42*, 439-451.

[27] S. C. Annedi, S. P. Maddaford, G. Mladenova, J. Ramnauth, S. Rakhit, J. S. Andrews, D. K. H. Lee, D. Zhang, F. Porreca, D. Bunton, L. Christies, *J. Med. Chem.* **2011**, *54*, 7408-7416.
[28] H. Huang, P. Martasek, L. J. Roman, B. S. Masters, R. B. Silverman, *J. Med. Chem.* **1999**, *42*, 3147-3153.
[29] M. L. Flinspach, H. Li, J. jamal, W. Yang, H. Huang, J. M. Hah, J. A. Gomez-Vidal, E. A. Litzinger, R. B. Silverman, T. L. Poulos, *Nat. Struct. Mol. Biol.* **2004**, *11*, 54-59.
[30] H. Ji, B. Z. Stanton, J. Igarashi, H. Li, P. Martasek, L. J. Roman, T. L. Poulos, R. B. Silverman, *J. Am. Chem. Soc.* **2008**, *130*, 3900-3914.
[31] W. M. Moore, R. K. Webber, G. M. Jerome, F. S. Tjoeng, T. P. Misko, M. G. Currie, *J. Med. Chem.* **1994**, *37*, 3886-3888.
[32] E. P. Garvey, J. A. Oplinger, E. S. Furfine, R. J. Kiff., F. Laszlo, B. J. Whittle, R. G. Knowles, *J. Biol. Chem.* **1997**, *272*, 4959-4963.
[33] W. Fast, D. Nikolic, R. B. Van Breemen, R. B. Silverman, *J. Am. Chem. Soc.* **1999**, *121*, 903-916.
[34] Y. Zhu, D. Nikolic, R. B. Van Breemen, R. B. Silverman, *J. Am. Chem. Soc.* **2005**, *127*, 858-868.
[35] W. K. Alderton, A. D. Angell, C. Craig, J. Dawson, E. Garvey, S. Moncada, J. Monkhouse, D. Rees, L. J. Russell, R. J. Russell, S. Schwartz, N. Waslidge, R. G. Knowles, *Br. J. Pharmacol.* **2005**, *145*, 301-312.
[36] K. McMillan, M. Adler, D. S. Auld, J. J. Baldwin, E. Blasko, L. J. Browne, D. Chelsky, D. Davey, R. E. Dolle, K. A. Eagen, S. Erickson, R. I. Feldman, C. B. Glaser, C. Mallari, M. M. Morrissey, M. H. Ohlmeyer, G. Pan, J. F. Parkinson, G. B. Phillips, M. A. Polokoff, N. H. Sigal, R. Vergona, M. Whitlow, T. A. Young, J. J. Devlin, *Proc. Natl. Acad. Sci. USA* **2000**, *97*, 1506-1511.
[37] L. Nagpal, M. H. Haque, A. Saha, N. Mukherjee, A. Ghosh, B. C. Ranu, D. J. Stuehr, K. Panda, *J. Biol. Chem.* **2013**, *288*, 19685-19697.
[38] E. D. Garcin, A. S. Arvai, R. J. Rosenfeld, M. D. Kroeger, B. R. Crane, G. Andersson, G. Andrews, P. J. Hamley, P. R. Mallinder, D. J. Nicholls, S. A. St-Gallay, A. C. Tinker, N. P. Gensmantel, A. Mete, D. R. Cheshire, S. Connolly, D. J. Stuehr, A. Aberg, A. V. Wallace, J. A. Tainer, E. D. Getzoff, *Nat. Chem. Biol.* **2008**, *4*, 700-707.
[39] B. J. Van der Schueren, M. W. Lunnon, B. E. Laurijssens, F. Guillard, J. Palmer, A. Van Hecken, M. Depré, F. H. Vanmolkot, J. N. de Hoon, *J. Clin. Pharmacol.* **2009**, *49*, 281-290.
[40] A. Hougaard, A. W. Hauge, S. Guo, P. Tfelt-Hansen, *Scand. J. Pain* **2013**, *4*, 48-52.
[41] P. Barbanti, G. Egeo, C. Aurilia, L. Fofi, D. Della-Morte, *Expert Opin. Investig. Drugs* **2014**, *23*, 1141-1148.
[42] H. Huang, H. Li, S. Yang, G. Chreifi, P. Martasek, L. J. Roman, F. L. Meyskens, T. L. Poulos, R. B. Silverman, *J. Med. Chem.* **2014**, *57*, 686-700.
[43] H. T. Do, H.-Y. Wang, H. Li, G. Chreifi, T. L. Poulos, R. B. Silverman, *J. Med. Chem.* **2017**, *60*, 9360-9375.
[44] H. T. Do, H. Li, G. Chreifi, T. L. Poulos, R. B. Silverman, *J. Med. Chem.* **2019**, *62*, 2690-2707.
[45] K. Narayanan, O. W. Griffith, *J. Med. Chem.* **1994**, *37*, 885-887.
[46] E. S. Furfine, M. F. Harmon, J. E. Paith, R. G. Knowles, M. Salter, R. J. Kiff, C. Duffy, R. Hazelwood, J. A. Oplinger, E. P. Garvey, *J. Biol. Chem.* **1994**, *269*, 26677-26683.
[47] N. M. Olken, K. M. Rusche, M. K. Richards, M. A. Marletta, *Biochem. Biophys. Res. Commun.* **1991**, *177*, 828-833.
[48] B. R. Babu, C. Frey, O. W. Griffith, *J. Biol. Chem.* **1999**, *274*, 25218-25226.
[49] N. Kobayashi, T. Higuchi, Y. Urano, K. Kikuchi, M. Hirobe, T. Nagano, *Biol. Pharm. Bull.* **1999**, *22*, 936-940.
[50] J. M. Park, T. Higuchi, K. Kikuchi, Y. Urano, H. Hori, T. Nishino, J. Aoki, K. Inoue, T. Nagano, *Br. J. Pharmacol.* **2001**, *132*, 1876-1882.
[51] A. Hamzé, J. Martinez, J.-F. Hernandez, *J. Org. Chem.* **2004**, *69*, 8394-8402.
[52] G. Li, H. Tajima, T. Ohtani, *J. Org. Chem.* **1997**, *62*, 4539-4540.
[53] S. Cantel, S. Desgranges, J. Martinez, J.-A. Fehrentz, *J. Pept. Sci.* **2004**, *10*, 326-328.
[54] J. Boström, A. Hogner, A. Llinas, E. Wellner, A. T. Plowright, *J. Med. Chem.* **2012**, *55*, 1817-1830.
[55] P. Pitasse-Santos, V. Sueth-Santiago, M. E. F. Lima, *J. Braz. Chem. Soc.* **2018**, *29*, 435-456.
[56] A. Hamzé, J.-F. Hernandez, P. Fulcrand, J. Martinez, *J. Org. Chem.* **2003**, *68*, 7316-7321.
[57] C. A. James, B. Poirier, C. Grisé, A. Martel, E. H. Ruediger, *Tetrahedron Lett.* **2006**, *47*, 511-514.
[58] J. E. Francis, L. A. Gorczyca, G. C. Mazzenga, H. Meckler, Tetrahedron Lett. **1987**, *28*, 5133-5136.
[59] J. M. Hevel, M. A. Marletta, *Meth. Enzymol.* **1994**, *233*, 250-258.
[60] C. Frey, K. Narayanan, K. McMillan, L. Spack, S. S. Gross, B. S. Masters, O. W. Griffith, *J. Biol. Chem.* **1994**, *269*, 26083-26091.
[61] K. Narayanan, L. Spack, K. McMillan, R. G. Kilbourn, M. A. Hayward, B. S. Masters, O. W. Griffith, *J. Biol. Chem.* **1995**, *270*, 11103-11110.
[62] H. Huang, P. Martasek, L. J. Roman, R. B. Silverman, *J. Med. Chem.* **2000**, *43*, 2938-2945.
[63] K. McMillan, B. S. Masters, *Biochemistry* **1993**, *32*, 9875-9880.
[64] M. Nakane, V. Klinghofer, J. E. Kuk, J. L. Donnelly, G. P. Budzik, J. S. Pollock, F. Basha, G. W. Carter, *Mol. Pharmacol.* **1995**, *47*, 831-834.
[65] G. C. Brown, C. E. Cooper, *FEBS Lett.* **1994**, *356*, 295-298.
[66] Y. Kato, Y. Miura, N. Yamamoto, N. Ozaki, Y. Oiso, *Diabetologia* **2003**, *46*, 1228-1233.
[67] L. Zhong, T. Tran, T. D. Baguley, S. J. Lee, A. Henke, A. To, S. Li, S. Yu, F.A. Grieco, J. Roland, P. G. Schultz, D. L. Eizirik, N. Roggers, A. K. Chartterjee, M. S. Tremblay, W. Shen, *Br. J. Pharmacol.* **2018**, *175*, 3470-3485.
[68] E. P. Garvey, J. A. Oplinger, G. J. Tanoury, P. A. Sherman, M. Fowler, S. Marshall, M. F. Harmon, J. E. Paith, E. S. Furfine, *J. Biol. Chem.* **1994**, *269*, 26669-26676.
[69] C. Moali, J.-L. Boucher, M.A. Sari, D.J. Stuehr, D. Mansuy, *Biochemistry* **1998**, *37*, 10453-10460.
[70] C. Wu, J. Zhang, H. Abu-Soud, D. K. Ghosh, D. J. Stuehr, *Biochem. Biophys. Res. Commun.* **1996**, *222*, 439-444.
[71] S. Ghosh, R. Gachhui, C. Crooks, C. Wu, M. P. Lisanti, D. J. Stuehr, *J. Biol. Chem.* **1998**, *273*, 22267-22271.
[72] H. M. Abu-Soud, R. Gachhui, F. M. Raushel, D. J. Stuehr, *J. Biol. Chem.* **1997**, *272*, 17349-17353.
[73] D. K. Ghosh, C. Wu, E. Pitters, M. Moloney, E. R. Werner, B. Mayer, D. J. Stuehr, *Biochemistry* **1997**, *36*, 10609-10619.
[74] M. M. Bradford, *Anal. Biochem.* **1976**, *72*, 248-252.
[75] D. J. Stuehr, M. Ikeda-Saito, *J. Biol. Chem.* **1992**, *267*, 20547-20550.
[76] M. Asfari, D. Janjic, P. Meda, G. Li, P. A. Halban, C. B. Wollheim, *Endocrinology* **1992**, *130*, 167–178.
[77] L. C. Green, D. A. Wagner, J. Glogowski, P. L. Skipper, J. S. Wishnok, S. R. Tannenbaum, *Anal. Biochem.* **1982**, *126*, 131-138.

Entry for the Table of Contents

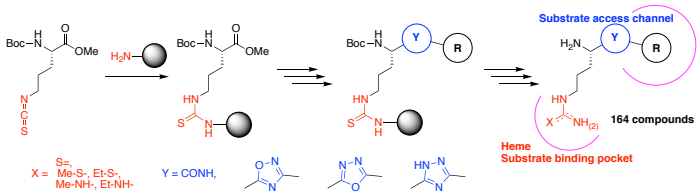

164 potential NO synthases inhibitors were prepared on solid support from a single thiocitrulline intermediate anchored by its side-chain. Most compounds inhibiting nNOS and/or iNOS with IC_{50} in the 1-50 μM range and with selectivity toward eNOS contained a *S*-Et-Itc moiety and mainly belonged to the dipeptide-like and 1,2,4-oxadiazole series. Selected inhibitors were found to significantly inhibit iNOS expressed in RAW264.7 and INS-1 cells.